Trop J Nat Prod Res, September 2025; 9(9): 4444 – 4459 ISSN 2616-0684 (Print)
ISSN 2616-0692 (Electronic)

Tropical Journal of Natural Product Research

Available online at https://www.tjnpr.org

Original Research Article

Structure-Based Discovery of Immunomodulators for Stunting Inspired by Caulerpin: A Rational Approach Targeting Immune Homeostasis

Jelita S.H. Hinonaung[1], Yeanneke L. Tinungki[1], Walter Balansa[2]*

[1]Department of Health, Politeknik Negeri Nusa Utara, North Sulawesi 95811, Indonesia
[2]Department of Fisheries and Maritime Technology, Politeknik Negeri Nusa Utara, North Sulawesi 95811, Indonesia

ARTICLE INFO

Article history:
Received 26 April 2025
Revised 21 August 2025
Accepted 22 August 2025
Published online 01 October 2025

ABSTRACT

Stunting remains a critical public health issue, affecting millions globally and hundreds of thousands in Indonesia annually, thus demanding innovative interventions. While immune dysfunction is implicated in the pathogenesis of stunting, it is often underemphasized in therapeutic strategies. This study leverages structure-based drug design and similarity searching to identify novel immunomodulators with potential application in stunting treatment. Initial molecular docking revealed that caulerpin (**1**), an algal alkaloid, exhibited promising binding to immune-related targets. However, its suboptimal drug-likeness prompted the use of SwissSimilarity structural search, leading to the identification of CPG-52852 (**7**), a TLR7 agonist. Compound **7** demonstrated strong predicted immunomodulatory properties via PASS analysis. Further similarity searching, using **7** as a query, identified imiquimod (**8**) and resiquimod (**9**), sharing similar imidazoquinolinone scaffold with **7**. Building upon the scaffold, de novo design of R848 with Metatox generated ten novel compounds (**12-21**) with predicted immunomodulatory activity nearly equal or improved drug-likeness with ADMET score of 0.25, 0.28, 0.28, and 0.32 for compounds **13**, **14**, **15**, and **17** compared to 0.29 for their parent molecule, R848. Unlike the TLR-7/8 agonist R848, compounds **13**, **14**, **15**, and **17** preferentially interacted with amino acid residues unrelated to the ones reported for the TLR-7/8 agonist, suggesting a distinct mechanism of action (e.g., antagonism or allosteric modulation). These allosteric modulators represent promising leads for treating immune dysfunction-related diseases, including stunting, where alternative mechanisms beyond direct agonism are needed.

Keywords: Caulerpin, Stunting, Immunomodulators, Toll-like receptor.

Introduction

Stunting remains a critical global health challenge, contributing to 45% of deaths in children under 5 years of age.[1] Globally, the prevalence of stunting is estimated at 22%;[2] however, this rate is significantly higher in Indonesia, reaching 36.4%.[3] Defined as being too short for one's age, specifically two standard deviations or more below the WHO Child Growth Standards median,[4,5] stunting affected approximately 149.2 million children under the age of 5 in 2020.[6] This condition is associated with increased mortality, impaired neurodevelopment, elevated chronic disease risk, and reduced productivity.[7] Recognizing the severity of this issue, one of the Sustainable Development Goals aims is to reduce stunting among children under five years by 40% by the year 2025.[7] Despite the potential of nutritional interventions to mitigate stunting, achieving consistent success with these methods has proven challenging.[8,9] Therefore, innovative, multisectoral, and evidence-based approaches are needed to effectively reduce the burden of stunting, particularly in low- and middle-income countries, including Indonesia.[8,9]

*Corresponding author. E mail: walter.balansa@fulbrightmail.org
Tel: +6282190626822

Citation: Hinonaung JSH, Tinungki YL, Balansa W. Structure-Based Discovery of Immunomodulators for Stunting Inspired by Caulerpin: A Rational Approach Targeting Immune Homeostasis. Trop J Nat Prod Res. 2025; 9(9): 4444 – 4459 https://doi.org/10.26538/tjnpr/v9i9.45

Official Journal of Natural Product Research Group, Faculty of Pharmacy, University of Benin, Benin City, Nigeria

One of such approaches is to address immune dysfunction. Malnutrition and stunting are not solely caused by inadequate food intake, but are also linked to recurrent infections and chronic inflammation, suggesting an underlying immune component.[10] Recent research suggests that immune dysfunction can be both a cause and a consequence of malnutrition. This is supported by meta-analyses demonstrating a correlation between a history of diarrhea in toddlers and an increased risk of stunting.[10] Chronic intestinal infections and inflammation can impair nutrient absorption and induce systemic inflammation, affecting cytokine levels and insulin-like growth factor-1 (IGF-1) formation.[11,12] Inflammatory pathways involving leptin, the leptin–adiponectin ratio, IGF-1, and gamma interferon (IFN-γ) may also contribute to stunting, particularly in children from Bangladesh.[13] These findings underscore the role of immune dysfunction in the cycle of clinical malnutrition.[8]

The marine alga *Caulerpa racemosa* has demonstrated both anti-inflammatory and immunomodulatory properties. While some studies attribute these effects to its constituent polysaccharides,[14] the immunomodulatory potential of caulerpin, a bis-indole alkaloid, remains largely unexplored. However, *in vivo* studies have shown that caulerpin can modulate the release of both pro- and anti-inflammatory cytokines in dextran sodium sulfate (DSS)-induced colitis mice by reducing TNF-α, IFN-γ, IL-6, IL-17, and NF-κB p65 while increasing IL-10, ultimately alleviating colon shortening and damage.[15] This suggests caulerpin as a promising natural product for the development of novel immunomodulatory compounds.

The known anti-inflammatory activity of caulerpin suggests it likely action via immunomodulation,[16] making it a potentially valuable lead for immunomodulatory targeted drug discovery. Toll-like receptors 7 and 8 (TLR7/8) represent key targets in immune regulation, implicated in various pathologies.[17] However, modulating TLR7/8 presents challenge as it can elicit complex or even detrimental immune responses

exemplified by TLR-7/8 agonists imidazoquinolinones administration on undernourished children.[17] This complexity underscores the need for precise TLR7/8 modulation, especially within the context of environmental enteric dysfunction (EED) associated with stunting – a condition characterized by chronic gut inflammation and immune dysregulation.[18] While targeting TLR7/8 in EED holds potential for restoring immune homeostasis,[17] it necessitates identifying specific modulators (e.g., antagonists or allosteric modulators) that can selectively resolve detrimental inflammation without causing adverse immune activation. Therefore, investigating caulerpin-derived or -inspired structures for their potential to act as specific TLR7/8 modulators represents a rational approach towards developing novel therapeutic strategies for EED and potentially other immune dysfunction disease.

This study aimed to leverage computational tools to screen for potential immunomodulators targeting key immune pathways implicated in stunting, with the ultimate goal of identifying lead compounds for further preclinical and clinical evaluation. By focusing on compounds with established safety profiles and favorable pharmacokinetic (PK) properties, the study aimed to accelerate the development of novel interventions to address the global burden of stunting.

Materials and Methods

Ligand and receptor preparation

The 3D structures of caulerpin (PubChem CID: 5326018), R848 (PubChem CID: 159603) were obtained from the PubChem database while R848 derivatives were generated from Metatox. Ligands were prepared for docking using PyRx (version 0.8), which involved adding polar hydrogen atoms, assigning pdbqt files and defining rotatable bonds. The crystal structure of the human heteromeric TLR-8 (PDB ID: 3W3J), which exhibits face-to-face interaction between two protomers, was downloaded from the Protein Data Bank. The receptor structure was prepared using PyRx, including removing water molecules, adding polar hydrogen atoms and treating the receptors as rigid during docking.

Molecular docking studies with key immune targets

Using Molsfot, drug likeness of all compounds was simulated.[19] Molecular docking was performed using AutoDock Vina (version 1.2.x) within PyRx (0.8 version).[19] A grid box encompassing the binding site of TLR-7/8 was defined with dimensions of 25 x 25 x 25 Å, centered at coordinates X = 22.8081, Y = 5.2868, and Z = 22.1206. These grid box parameters were chosen to encompass both the orthosteric (site 1) and allosteric binding sites identified by Zheng *et al*. (2019).[20] The exhaustiveness parameter was set to 8 to ensure a thorough search of the conformational space. For each ligand, the top 10 poses were generated, and the pose with the lowest binding energy (ΔG in kcal/mol) was selected for further analysis. The docking simulations were performed for caulerpin, R848 and its MetaTox generated derivatives.

Drug likeness Molsoft ICM Chemoinformatics tools

Drug-likeness was assessed using Molsoft ICM Chemoinformatics tools (ICM v.3.8, Molsoft L.L.C., San Diego, CA, USA). The ICM Drug-likeness Score, which considers a molecule's physicochemical properties (e.g., molecular weight, LogP, hydrogen bond donors/acceptors) and structural features to predict its similarity to known drugs, was calculated for caulerpin and the selected compounds. A higher ICM Drug-likeness score indicates a greater similarity to known drugs, suggesting a higher probability of exhibiting drug-like behavior.

SwissSimilarity analysis

The resulting compounds from the SwissSimilarity and MetaTox search were then subjected to PASS (Prediction of Activity Spectra for Substances) analysis.[21] PASS utilizes a sophisticated algorithm that analyzes the structural features of a compound and compares them to a database of known bioactive molecules to predict its potential biological activities.[21] This analysis generates Pa and Pi scores, representing the probabilities of a compound being active or inactive for a given activity, respectively. The online PASS server was used to predict the probabilities of "Pa" (probability to be active) and "Pi" (probability to be inactive) for various immunomodulatory activities, including, but not limited to, immunostimulant, anti-inflammatory, and cytokine modulating activities. Compounds with Pa > Pi for multiple relevant immunomodulatory activities were selected for further investigation because the main aim of this study was to discover compounds with immunomodulatory activity. The query was addressed to combined 2D and 3D ChEMBL drug candidates in clinics. To further investigate the potential for identifying structurally related compounds with similar immunomodulatory activity, a scaffold-based similarity search was conducted, focusing on 2D scaffolds present within ChEMBL's collection of drug candidates currently in clinical trials utilizing the SwissSimilarity platform.[21]

MetaTox analysis

To generate imidazoquinolinone derivatives,[22,23] the cdx file of imidazoquinolinone bearing molecule was uploaded to MetaTox webtool.[24] The cut-off was set with probability activity (Pa) larger than probability inactive (Pi) (Pa>Pi), generating >30 metabolites through phase I and II reactions. The representative products from various reactions were further evaluated in PASS analysis to evaluate their immunomodulating activity.

ADMET analysis

A quantitative ADMET scoring function was developed utilizing 18 distinct endpoints (Table 1). In this scheme, a binary classification assigned q = 1 for 'beneficial' properties and q = 0 for 'harmful' ones. Predicted values for harmful endpoints, including Ames, AO, CARC, specific CYP inhibitors (CYP1A2, CYP2C9, CYP2D6, CYP2C19, CYP3A4), CYPPRO, hERG blockers, OCT2 inhibitors, and P-gp inhibitors were transformed to q = 0 (e.g., hERG+). Conversely, beneficial predictions (e.g., hERG–) were coded as q = 1. The composite ADMET score was subsequently normalized to a 0 - 1 scale (0 = least desirable, 1 = most desirable) relative to scores of oral drugs in DrugBank.[25]

PASS analysis

The resulting compounds from the SwissSimilarity search were then subjected to PASS (Prediction of Activity Spectra for Substances) analysis.[27] PASS utilizes a sophisticated algorithm that analyzes the structural features of a compound and compares them to a database of known bioactive molecules to predict its potential biological activities. This analysis generates Pa and Pi scores, representing the probabilities of a compound being active or inactive for a given activity, respectively. The online PASS server was used to predict the probabilities of "Pa" (probability to be active) and "Pi" (probability to be inactive) for various immunomodulatory activities, including, but not limited to, immunostimulant, anti-inflammatory, and cytokine modulating activities. Compounds with Pa > Pi for multiple relevant immunomodulatory activities were selected for further investigation.

ISSN 2616-0684 (Print)
ISSN 2616-0692 (Electronic)

Table 1: The ADMET properties used in the calculation of the ADMET-score

End points	W_1	W_2	W_3	W_i
Ames mutagenicity	0.7142	0.8430	1.0	0.6021
Acute oral toxicity	0.7052	0.8320	1.0	0.5867
Caco-2 permeability	0.5004	0.7680	0.8	0.3074
Carcinogenicity	0.8404	0.8160	1.0	0.6857
CYP1A2 inhibitor	0.5839	0.8147	0.5	0.2379
CYP2C19 inhibitor	0.6668	0.8054	0.5	0.2685
CYP2C9 inhibitor	0.7396	0.8020	0.5	0.2966
CYP2C9 substrate	0.6759	0.7790	0.5	0.2633
CYP2C9 inhibitor	0.6617	0.8550	0.5	0.2829
CYP2D6 substrate	0.5926	0.7750	0.5	0.2296
CYP3A4 inhibitor	0.6630	0.6450	0.8	0.3421
CYP3A4 substrate	0.5097	0.6600	0.8	0.2691
CYP inhibitory promiscuity	0.5856	0.8210	1.0	0.4808
hERG inhibitor	0.5049	0.8040	1.0	0.4059
Human intestinal absorption	0.7821	0.9650	1.0	0.7548
Organic cation transporter protein 2 inhibitor	0.6345	0.8080	0.5	0.2564
P-gp inhibitor	0.5422	0.8610	0.8	0.3735
P-gp substrate	0.5399	0.8020	0.8	0.3464

Results and Discussion

While TLR7/8 receptors are being actively pursued for potential treatments of autoimmune diseases such Lupus,[28] its application in stunting is limited, complicated by observations of mixed responses to TLR7/8 agonists.[17] Building on prior work exploring scaffold modification for TLR antagonism,[22,29,30] but taking a novel natural product-inspired approach (caulerpin), the present study employed an *in silico* tools (Docking, PASS, SwissSimilarity, MetaTox) to identify and characterize potential aminoquinoline-based TLR7/8 modulators (antagonistic or allosteric modulators) aimed at addressing immune dysfunction in stunting.

Molecular docking against TLR7/8 receptors

To evaluate the immunomodulating potential of caulerpin, a bis-indole alkaloid isolated from *Caulerpa racemosa*, *in silico* methods, including molecular docking against Toll-like receptors 7 and 8 (TLR-7/8) and assessment of drug-likeness properties were employed. Molecular docking simulations predicted a strong binding affinity for caulerpin to the TLR-7/8 receptor complex, yielding a binding energy of -10.2 kcal/mol. This predicted affinity surpasses those calculated for several known TLR-7/8 agonists, which ranged from -7.5 to -9.1 kcal/mol under identical docking conditions. Analysis of the predicted binding mode indicated that caulerpin interacts with a distinct set of amino acid residues compared to the TLR-7 agonist MHV730 and the dual TLR-7/8 agonists R848 and Orto-amine (Table 2). However, some overlap in interacting amino acid residues (Tyr597, Tyr468, Ala571, Pro264, Phe320) was observed when compared to other docked ligands such as hybrid 2 and meta-amine (Table 2). Importantly, similar to most reference agonists (excluding MHV730), caulerpin was predicted to bind within Site 1, which is recognized as the orthosteric agonist binding site of the TLR-7/8 receptor.[31] These computational findings collectively suggest that caulerpin possesses the potential to act as a TLR-7/8 agonist.

Table 2: Molecular docking of caulerpin and four known TLR-7/8 agonists

Molecule	PDB ID: 3W3J (Kcal/mol)	Amino acid residues with the strongest binding (PDB 3W3J)
Caulerpin **(1)**	-10.2	Arg375, Tyr468, His469, Tyr597, Tyr597 (hydrogen), Ala571, Tyr597, Phe467, Ala571, Pro264, Pro264, Ala571 (hydrophobic).
R848 **(2)**	-7.5	Arg541, His566, Asn540, Ser516, Ser516 (Hydrogen)
Hybdrid-2 **(3)**	-7.8	Tyr597 (Hydrogen), Ala571, Phe320, Pro264, Pro264, Phe265, Phe320, Tyr468, Ala571, Pro264, Ala571 (hydrophobic)
Para-amine **(4)**	-8.7	Ser207, Asn466 (Hydrogen), Asp252 (Electrostatic), Asn466, Phe228, Phe228, Phe228 (Hydrophobic)
Meta-amine **(5)**	-9.1	Asn466 (Hydrogen), Phe320, Phe461, Pro264, Phe265, Phe320, Tyr468, Tyr468, Ala571, Pro264, Ala571, Ala571 (Hydrophobic)
Ortho-amine **(6)**	-8.5	

Despite the favorable binding predictions, subsequent *in silico* analysis of physicochemical and drug-like properties highlighted potential issues for caulerpin as a drug candidate. Chemoinformatic analysis (Molsoft) yielded a calculated MolLogP of 4.09 for caulerpin, indicating higher lipophilicity compared to the reference agonists (MolLogP range: 1.89 – 3.80, Table 3). Furthermore, caulerpin exhibited a larger total surface area (TSA: 400 Å²) than the reference agonists (e.g., average or representative agonist TSA: 364 Å²), a factor that can influence solubility and membrane permeation. Critically, established drug-likeness models predicted poor drug-like characteristics for caulerpin, contrasting sharply with the favorable drug-likeness scores obtained for the benchmark TLR-7/8 agonists (Table 4, Figure 1). While TLR-7/8 agonists hold promise for immunotherapy, challenges such as variable immunological responses necessitate the development of novel modulators, potentially including agonists or allosteric agents with improved profiles for specific applications.[17] Therefore, the divergence between caulerpin's strong predicted binding affinity and its suboptimal drug-like properties suggests that a structure-based drug design strategy, aimed at preserving key pharmacophoric features for TLR-7/8 interaction while enhancing physicochemical characteristics, represents a promising avenue for future investigation.

Table 3: Drug-likeness measured by Molsoft

Property	Caulerpin (1)	R848 (2)	Hybrid-2 (3)	Para-amine (4)	Meta-amine (5)	Ortho-amine (6)	Notes/Significance
Molecular Weight	398.13	359.21	314.17	359.21	359.21	317.29	< 500 desirable
HBA	4	3	4	3	3	3	≤ 10 acceptable
HBD	2	4	3	4	4	3	≤ 5 generally desirable
MolLogP	4.09	3.72	1.89	3.88	3.80	3.38	≤ 5 desirable -Lipophilicity
MolLogS	-4.31	-3.83	-1.95	-4.03	-3.83	-3.19	Water Solubility, the closer it is to 0, the easier it is to dissolved, 25-6
MolPSA (A^2)	62.99	62.38	65.23	62.38	62.38	57.18	Helpful in binding affinity
MolVol	403.47	364.54	321.82	364.23	364.47	329.37	Helpful to bind
Drug likeness score	-1.08	0.66	0.47	0.15	0.55	0.36	Higher is better

Table 4: Drug likeness and bioactivity of 10 out of 53 compounds analyzed using PASS analysis

Code	Drug likeness	Immunomodulating activity	Bioactivity (possibility of active)
CHEMBL49642 (indibulin)	1.14	negative	Antiallergic (0.60) Antineoplastic (0.55)
CHEMBL3542265	0.75	negative	Reproductive dysfunction (0.67)
CHEMBL10188 (talnetant)	1.01	negative	Taurine/amine dehydrogenase inhibitor (0.764)
CHEMBL2105060 (moxaverine)	0.84	negative	Cyclic AMP phosphodiesterase inhibitor (0.77)
CHEMBL9960	0.59	negative	Taurine dehydrogenase inhibitor (0.781)
CHEMBL1618279 (revaprazan)	1.39	negative	Antidyskinetic (0.542)
CHEMBL290429 (Carfentanil)	1.25	negative	Anesthetic general (0.962)
CHEMBL549344/ CPG-52852	0.78	positive	Immunomodulator (0.954); Cytokine production stimulant (0.950); Cytokine modulator (0.873); Interferon alpha agonist (0.78)
CHEMBL279433	0.96	negative	Farnesyltransferase inhibitor (0.809)
CHEMBL2181927	1.25	negative	Antihypertensive (0.723)

To identify potential immunomodulatory compounds with structural similarity to caulerpin (**1**), a similarity search was performed using SwissSimilarity, a platform known for its diverse 2D and 3D similarity metrics.[21] Specially the query was addressed to combined 2D and 3D ChEMBL drug candidates in clinics (Figure 3). This approach yielded 155 compounds possessing various structural motifs, including fused bicyclic/polycyclic systems, nitrogen-containing heterocycles, sulfonamides, and carboxylic acid derivatives. To prioritize compounds with immunomodulatory potential, we further filtered this set using PASS (Prediction of Activity Spectra for Substances) analysis (Table 4).

PASS analysis and identification of CPG-52852

PASS analysis indicated that the majority of molecules exhibited predicted bioactivities unrelated to immunomodulation, displaying a diverse range of potential effects including antiallergic, anesthetic, antihypertensive, and antitumor activities. In contrast, CPG-52852 demonstrated a high probability of immunomodulatory activity, with predicted activity (Pa) values of 0.954 for immunomodulation, 0.950 for cytokine production stimulation, and 0.873 for cytokine modulation (Table 5). These findings are consistent with reports from the National Center for Biotechnology Information (NCBI) indicating that CPG-52852 acts as a TLR7 agonist. The NCBI reports that CPG-52852 is currently undergoing Phase II clinical trials evaluating its antitumor and immunostimulatory properties.[32] Therefore, based on these findings, CPG-52852 was identified as the lead compound in this study.

ISSN 2616-0684 (Print)
ISSN 2616-0692 (Electronic)

To further investigate the potential for identifying structurally related compounds with similar immunomodulatory activity, a scaffold-based similarity search was conducted, focusing on 2D scaffolds present within ChEMBL's collection of drug candidates currently in clinical trials.

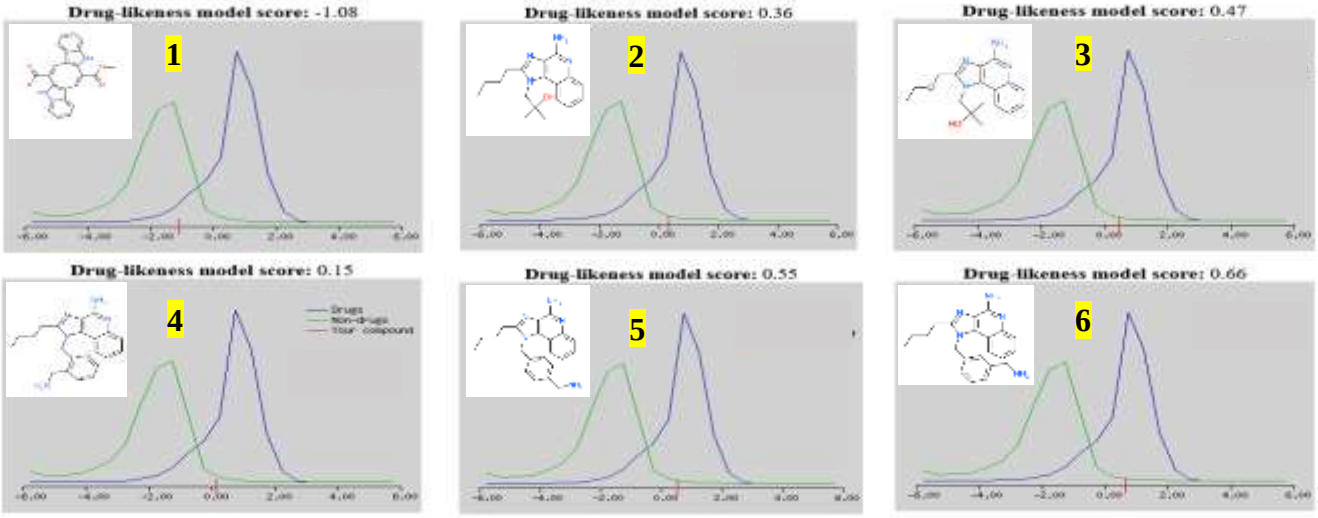

Figure 1: Drug-likeness model score for caulerpin (**1**) and TLR7/8 agonists (**2-6**) with blue, green and red lines indicating the model for drugs, non-drugs and compounds **1-6**, respectively

Table 5: Immunomodulating activity of the hit compound (CPG-52852, imiquimod and resiquimod and other known TLR-7/8 agonists

Code	Drug likeness	Binding affinity (Kcal/mol) PDB ID: 3W3J	Immunomodulating Activities, Probability active (Pa)					
			1 (Pa)	2 (Pa)	3 (Pa)	4 (Pa)	5 (Pa)	6 (Pa)
CPG-52852 (**6**)	0.77	-8.8	0.954	-	0.950	-	-	0.873
Imiquimod (**7**)	0.64	-7.7	0.983	0.931	0.932	0.688	0.815	0.778
Resiquimod (**8**)	0.47	-8.9	0.770	0.759	-	-	-	-
Orto-amine (**9**)	0.15	-8.5	0.726	0.726	0.462	-	-	-
Meta-amine (**10**)	0.55	-9.1	0.771	0.756	0.555	-	-	-
Para-amine (**11**)	0.15	-8.7	0.779	0.756	0.555	-	-	-
MHV370								
R848	0.47	-7.5	0.983	0.931	0.780	0.778	0.815	0.932

Note: 1 = immunomodulator, 2 = interferon alpha agonist, 3 = interferon agonist, 4 = immunostimulant, 5 = cytokine production stimulant, 6 = cytokine modulator.

Using the SwissSimilarity platform, this analysis identified two known immunomodulators, imiquimod and resiquimod, as exhibiting significant structural similarity to CPG-52852. Notably, imiquimod and resiquimod represent the most widely used and investigated topical TLR agonists,[20,33] that have proven effective in curing viral and superficial cancer with favorable side effects.[33] Intriguingly, they share the same scaffold, the imidazoquinolinone core, suggesting the importance of this scaffold for the development of new derivatives that may activate both the innate and adaptive immune system.

Thus, a PASS analysis of CPG-52852, imiquimod, and resiquimod was conducted, and their predicted bioactivity was compared with that of other compounds containing imidazoquinolinone scaffold, such as R848, meta-amine, para-amine, and ortho-amine. The results indicated that, despite slight differences in the level of predicted activity, these imidazoquinolinone compounds all exhibited immunomodulating activities, including acting as immunomodulators, interferon alpha agonists, interferon agonists, immunostimulants, cytokine production stimulants, and cytokine modulators (Table 4). Specifically, CPG-52852 and resiquimod demonstrated high predicted activity (Pa) for immunomodulation (0.954, 0.983), cytokine production stimulation (0.950, 0.932), and cytokine modulation (0.873, 0.931), respectively (Table 5). On the other hand, imiquimod, para-amine, meta-amine, and ortho-amine showed slightly lower predicted immunological activity, with Pa values of 0.770, 0.756, 0.771, and 0.779, respectively for immunomodulation, and 0.759, 0.726, 0.756, and 0.462, respectively for interferon-alpha agonist (Table 5).

These results support the hypothesis that molecules bearing the imidazoquinolinone scaffold possess a range of immunological bioactivities. This suggests that generating derivatives with the imidazoquinolinone scaffold using MetaTox, for example, can lead to the discovery of molecules with immunomodulating activities. Although glucuronidated and sulfated products are often considered less active despite demonstrating improved pharmacokinetic profile,[34] growing evidence suggests improved bioactivity even for the glucuronidated and sulfated metabolites.[35,36] Hence, an increasing number of studies have employed MetaTox to generate metabolites, not only for assessing their potential environmental toxicity, but also for evaluating the bioactive potential of natural products compounds.[20,37–41]

MetaTox analysis

MetaTox analysis predicted 31 metabolites of R848 (Figure 2), ten of which were selected for further evaluation based on their potential immunomodulatory activity (Figure 2, Table 4). These included activity as toll-like receptor (TLR) agonists (metabolites 16, 18, and 24), cytokine production stimulants (metabolites 13, 15, and 17), toll-like

ISSN 2616-0684 (Print)
ISSN 2616-0692 (Electronic)

receptor antagonists (metabolites 13, 15, and 27), and immunostimulants (metabolites 5, 13, 17, 21, 23, and 27). These ten metabolites represent diverse biotransformation products of R848, including alkyl side chain elimination (metabolite 5, corresponding to R848-El, **12**), *N*-oxidation (metabolite 13, R848-Nox, **13**), side chain modification (metabolite 15, R848-Mod, **14**), O-dealkylation (metabolite 16, R848-ODet, **15**), O-deethylation and hydroxylation (metabolite 17, R848-ODetHyd, **16**), O-glucuronidation (metabolite 18, R848-Gluc, **17**), hydroxylation and oxidation (metabolite 21, R848-HydOx, **18**), aromatic hydroxylation (metabolite 23, R848-ArHyd, **19**), sulfation (metabolite 24, R848-Sulf, **20**), and *N*-oxidation (metabolite 27, R848-NOx, **21**) (Figure 4).

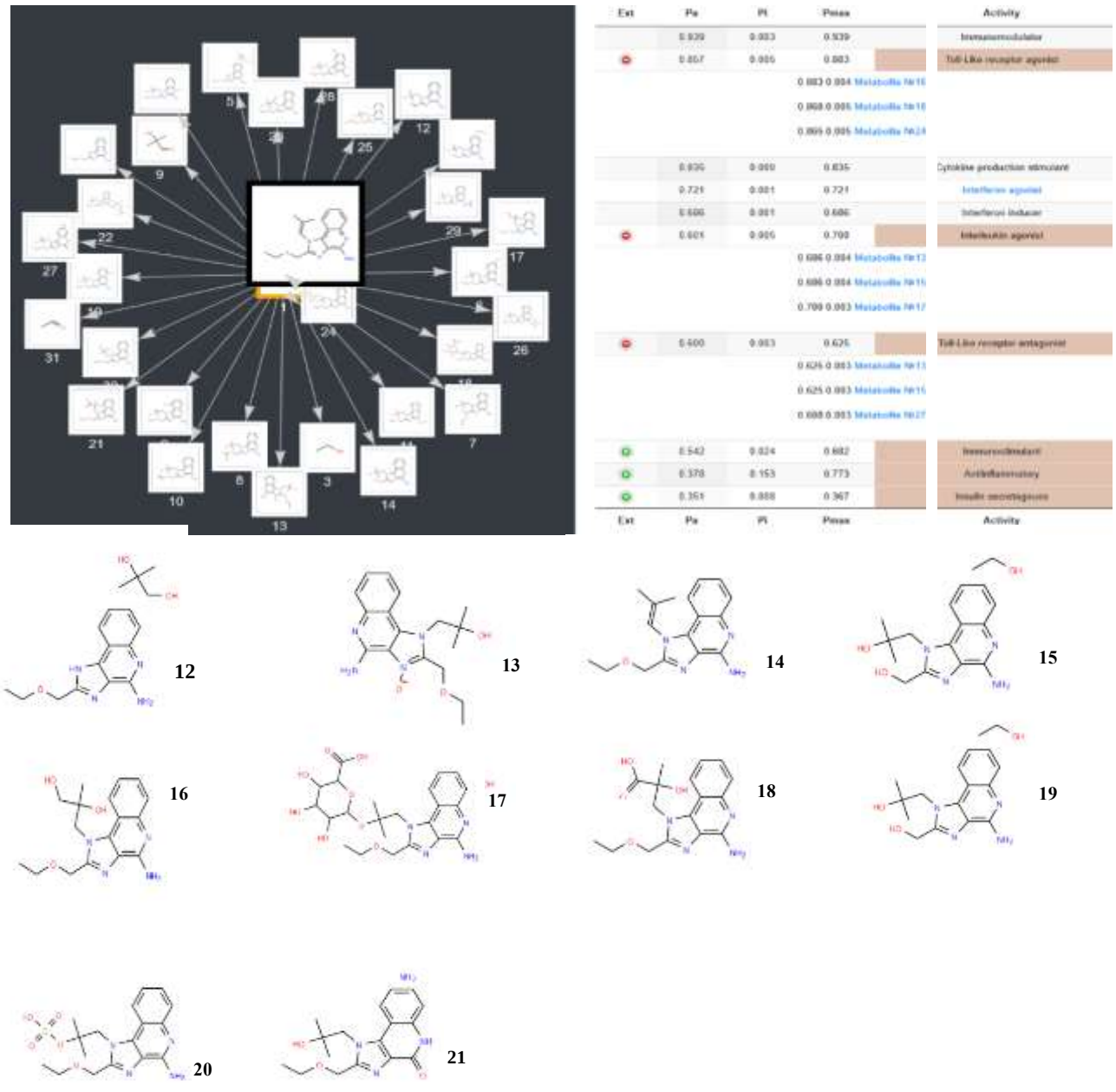

Figure 2: Structures of 10 out of 31 metabolites generated from R848 using Metatox Analysis
https://www.way2drug.com/metatox/view_path_smirks.php?id_task=67d55ca390688

ISSN 2616-0684 (Print)
ISSN 2616-0692 (Electronic)

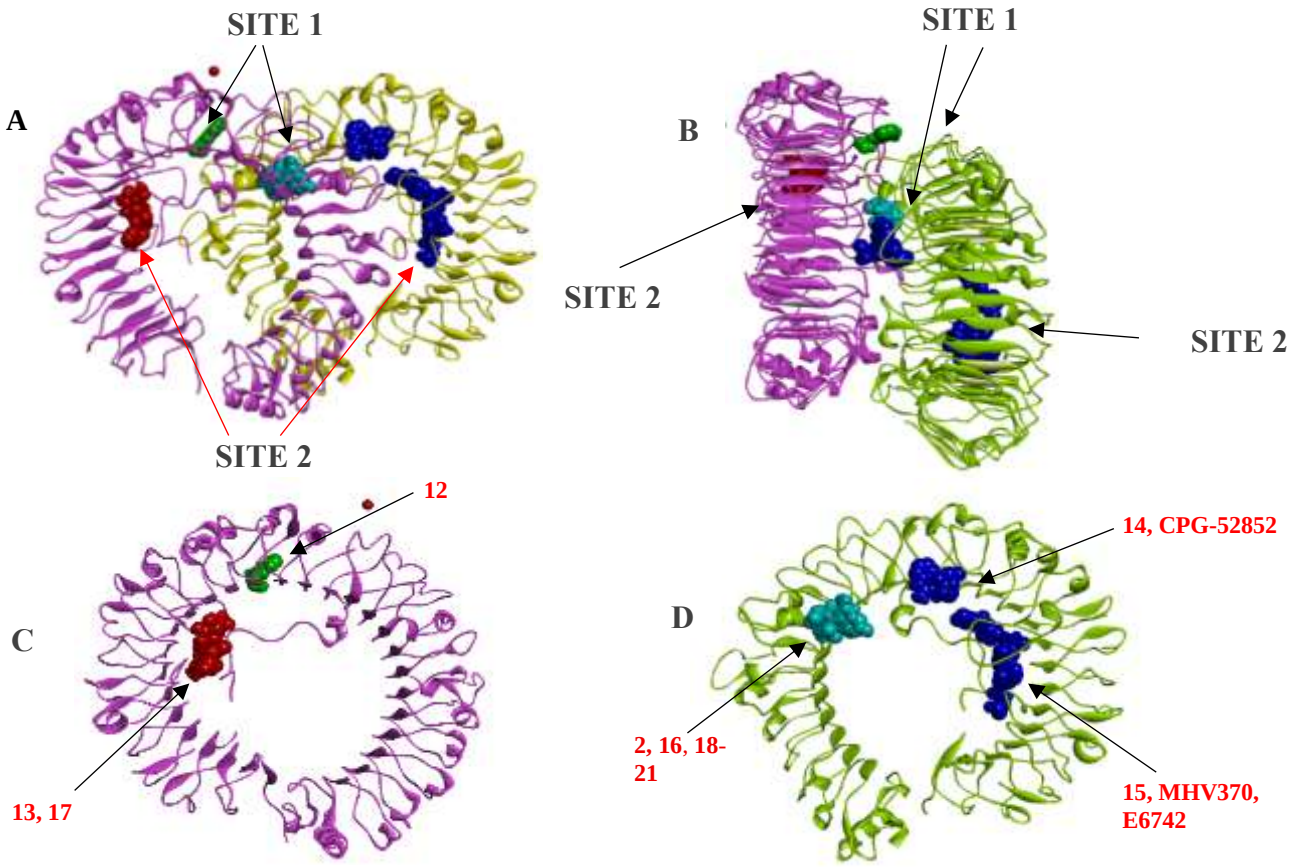

Figure 3: Crystal structure of the TLR-8 dimer (PDB ID: 3W3J) in front (Panel A) and side (Panel B) views. Key interaction sites are highlighted: Site 1 involves compound **12** (Panel C) and TLR-7/8 agonist (2) and its analogues **16**, **18-21** (Panel D), while Site 2 involves analogues **13**, **17** (Panel C) and **14** and TLR-7 antagonist (CPG), **15** and TLR-7 antagonists (MHV370, E6742) (Panel D).[51,52]

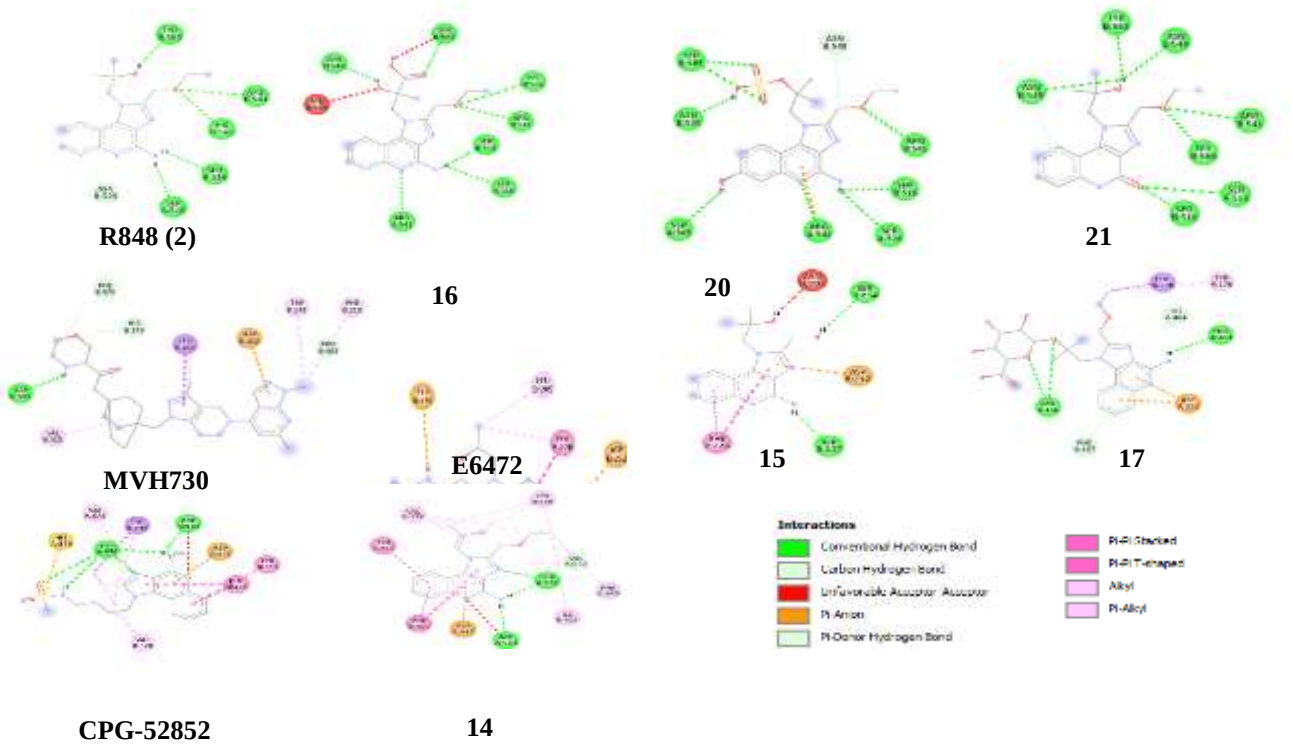

Figure 4: Visualization of receptor-ligand interactions showing putative binding sites within the TLR-7/8 receptor. Docking poses compare the reference agonists between (R848 and CPG-52852) and compounds **16**, **20-21** (Panel A), between antagonists (MHV-730, E6472) and compounds **15**, **17** (Panel B) as well as between CPG-52852 and compound **14** (Panel C), illustrating two different subregions in the orthosteric agonist site (Panels A, C) and one antagonistic/allosteric modulator site (Panel B).

ISSN 2616-0684 (Print)
ISSN 2616-0692 (Electronic)

As expected, the Metatox analysis revealed that, similar to R848, all derivatives (**12-21**) exhibited immunological activities, although with varying probabilities of being active (Pa) and different profiles of related activities (Table 6). While compounds **12**, **15**, and **16** showed a more limited range of two to three activities, including those of immunomodulators (Pa = 0.975, 0.882, 0.758), interferon alpha agonists (Pa = 0.896, 0.000, 0.626), and immunostimulants (Pa = 0.790, 0.825, 0.871), respectively. The remaining derivatives demonstrated more comprehensive immunomodulating activities (Table 6). This result consistently demonstrates that compounds with imidazoquinolinone scaffolds particularly have strong immunomodulating potential. This result corroborates with recent discovery by Wang *et al*.[42] Who reported several imidazoquinolinone as TLR-7/8 agonists capable of reactivating immunosuppressive macrophages to produce inflammatory cytokines, increasing phagocytosis of tumor cells and enhancing T cell activation and proliferation.

Table 6: Immunomodulating activity of the hit compound (CPG-52852, imiquimod and ersiquimod and other known TLR-7/8 agonists

Code	Drug likeness	Binding affinity (Kcal/mol) PDB ID: 3W3J	Immunomodulating Activities, Probability Activate (Pa)					
			1 (Pa)	2 (Pa)	3 (Pa)	4 (Pa)	5 (Pa)	6 (Pa)
R848 **(2)**	0.47	-7.5	0.932	0.983	-	0.780	0.815	0.932
R848-El **(12)**	-0.21	-7.0	0.975	0.790	-	0.896	-	-
R848-Nox **(13)**	0.53	-8.1	0.940	0.886	0.673	0.760	0.578	0.764
R848-Mod **(14)**	0.39	-8.7	0.959	0.915	0.710	0.776	0.678	0.802
R848-ODet**, (15)**	0.26	-7.5	0.882	0.825	-	-	-	-
R848-ODetHyd **(16)**	0.31	-7.8	0.758	0.871	-	0.626	-	-
R848-Gluc **(17)**	0.35	-9.1	0.975	0.790	0.790	0.896	0.551	-
R848-HydOx **(18)**	0.69	-8.0	0.874	0.907	0.498	0.614	0.485	0.622
R848-ArHyd **(19)**	0.29	-7.5	0.673	0.771	0.680	0.544	-	-
R848-Sulf **(20)**	-0.34	-7.9	0.944	0.943	-	0.738	0.701	0.675
R848-NOx **(21)**	-0.23	-7.7	0.866	0.899	0.540	0.633	0.510	0.502

Note: 1 = immunomodulator, 2 = interferon alpha agonist, 3 = interferon agonist, 4 = immunostimulant, 5 = cytokine production stimulant, 6 = cytokine modulator.

Table 7: Binding affinity, binding site and amino acid residues of CPG-52852, imiquimod and resiquimod and other known TLR-7/8 agonists

Compound Code	Binding affinity PDB ID: 3W3J	Binding site		Amino acid residues against Tlr_7 (PDB ID: 3W3J (7) and Tlr_8 (PDB: 5MGH (8)
R848 **(2)**	-6.9	Site 1	-	Arg541, His566, Tyr563, Ser516, Ser516, Asn539 (Site1, 3W3J/TLR-8).
R848-El **(12)**	-8.6	Site 1	-	Phe405, Phe405, Thr574, Val378, Val573, (Site 1, 3W3J/TLR-8).
R848-Nox **(13)**	-7.0	-	Site 2	Trp179, Ser207, Ser465, Ser465, Phe228, Phe228 (Site 2, 3W3J/TLR-8).
R848-Mod **(14)**	-6.7	Site 1	-	Ile403, Phe346, Phe405, Phe405, Tyr353, Tyr348, Tyr348, Tyr348, Val378, Val378, Val573, Val573 Val573 (Site 1, 3W3J)
R848-ODet**, (15)**	-6.1	-	Site 2	Asp252, Phe228, Phe228, Phe228, Ser207, Ser254 (Site 2, 3W3J/TLR-8)
R848-ODetHyd **(16)**	-6.8	Site 1	-	Arg541, Asn540, Asn540, His566, Ser516, Ser516, Tyr563 (Site 1, 3W3J/TLR-8)
R848-Gluc **(17)**	-9.2	-	Site 2	Asn466, Asn466, Asp252, Asp252, His464, Phe467, Phe228, Pro463, Tyr176 (Site 2, 3W3J/TLR-8).
R848-HydOx **(18)**	-7.7	Site 1	-	Arg541, Arg541, Asn540, His566, Ser516, Ser516, Ser565 (Site 1, 3W3J/TLR-8).
R848-ArHyd **(19)**	-6.6	Site 1	-	Arg541, Asn540, Asn540, His566, Ser516, Ser516, Ser565, Tyr563 (Site 1, 3W3J/TLR-8).
R848-Sulf **(20)**	-7.5	Site 1	-	Arg541, Arg541, Arg541, Arg541, Arg541, Asn539, Asn540, Ser565, Ser565, Ser565, Ser516, Ser516, Ser565, Unk1, Unk1, (Site 1, 3W3J/TLR-8).
R848-NOx **(21)**	-6.9	Site 1	-	Arg541, Asn539, Asn539, Asn540, His566, Ser516, Ser516, Tyr563, (Site 1, 3W3J/TLR-8).
MHV370	-10.8	-	Site 2	Asp252, Asp343, His373, Leu250, Leu250 Phe210, Phe470, Pro463, Trp179, Trp179, Val315 (Site 2, 3W3J/TLR-8).
E6742	-8.6	-	Site 2	Asp252, Leu205, Phe228, Phe228, Phe228, Tyr176, UNK1 (Site 2, 3W3J/TLR-8).

CPG-52852	-8.8	Site 1	-	Asp543, Asp545, His576, Phe405, Phe405, Phe405, Thr574, Thr574, Thr754, Thr754, Tyr348, Tyr348, Tyr353, Val378, Val378, Val573 (Site 1, 3W3J/TLR-8).

Furthermore, the present data indicate that compounds **13** and **18** exhibit a distinct immunomodulatory profile compared to the TLR-7/8 agonist R848. Specifically, *in silico* activity predictions (Table 6) reveal that both compounds **13** and **18** are characterized by a broader spectrum of immunomodulatory activities, encompassing six distinct categories including immunomodulation, cytokine production stimulation, interferon-alpha agonism, immunostimulant, interferon agonism, and cytokine modulation. In contrast, while R848 is predicted to possess activity across five of these categories, it notably lacks predicted interferon agonist activity. This differential profile suggests that compounds **13** and **18** may engage TLR-7/8 signaling pathways in a manner that elicits a broader or qualitatively different immune response compared to the canonical agonist R848, further supported by their differing binding affinity, binding site and amino acid residues (Table 7).

To assess the potential for *in vivo* applicability, the predicted Absorption, Distribution, Metabolism, Excretion, and Toxicity (ADMET) properties of the synthesized compounds were evaluated using established *in silico* methodologies.[25] Employing a panel of 18 ADMET endpoints (Table 8), a composite ADMET score for each compound was derived. This score, ranging from 0 (less favorable) to 1 (more favorable), serves as a predictive index of oral drug in Data Bank,[25] based on binary categorization of each endpoint (Table 9). Interestingly, while compounds **13 - 16** exhibited slightly lower ADMET scores (0.26 - 0.28), indicating potentially less favorable overall drug-like characteristics, derivatives 12, and specifically 14 - 17 and 20 - 21, demonstrated ADMET scores exceeding that of the parent molecule R848. This suggests that these latter derivatives may possess improved physicochemical properties associated with enhanced oral bioavailability and reduced potential for adverse effects compared to R848, warranting further investigation as potential therapeutic leads.

Analysis of predicted ADMET properties revealed potential improvements in the safety profiles of specific derivatives, notably compounds **17**, **19** and **20** with ADMET score of 0.32 compared to 0.29 for the parent molecule R848 (Table 9). Specifically, these derivatives lacked the predicted mutagenicity and CYP1A2 inhibition issue associated with R848, although this predicted improvement coincided with a potential decrease in absorption parameters (Table 10). Nevertheless, as the need for new antagonists or allosteric modulators for TLR-7/8 increases,[29,43] binding modes to the allosteric sites of TLR-7/8 receptors is crucial for discovering potent and safe TLR-7/8 modulators. While structurally distinct, this concept of achieving altered pharmacological profiles through modification conceptually aligns with observations where metabolic transformations have been shown to modulate bioactivity particularly various glucuronidated containing molecules.[20,34–41]

However, the present findings differ from specific prior reports. For instance, Tojo *et al*. (2020)[43] identified the substitution of 8-oxo group as a key determinant for achieving TLR7 antagonism within the 8-oxoadenine derivatives. In contrast, results from the present study suggest that diverse substitutions on the core imidazoquinolinone scaffold can yield molecules with potentially different mechanisms of action (e.g., antagonism or allosteric modulation) compared to the parent agonist particularly for the predicted compounds **13**, **15** and **17** (Figure 3). This highlights the possibility of generating functionally distinct TLR7/8 modulators through varied structural modifications, offering alternative strategies for developing therapeutics potentially suitable for conditions like stunting.

Prediction of orthosteric and allosteric binding modes

To elucidate the structural basis for potential differences in immunomodulatory activity, molecular docking simulations of R848 and its derivatives (compounds **12-21**) were performed using the crystal structure of the human TLR7/8 heterodimer (PDB ID: 3W3J) as a representative due to the close similarity between TLR-7 and TLR-8.[29] Also, the residues constituting the orthosteric or active sites of TLR-7 an TLR-8 are well conserved, resulting in both TLR-7 and TLR-8 using the same binding site.[44] The structure of TLR-7/8 reveal two key ligand binding sites: the canonical orthosteric site (Site 1), located at the dimer interface where agonists like R848 bind, and a distinct allosteric site (Site 2), situated peripherally (Figure 3A, 3B) where antagonists such as MHV370 binds.[43,45]

Our docking results, consistent with previous findings,[43] indicate distinct binding modes for the compounds. Derivatives 12, 14, 16, and 18 - 21, like the parent agonist R848, preferentially bind within the orthosteric Site 1 (Figures 3C, 3D), interacting with key residues like Arg341, His566, Ser516, and Asn539 (Table 7, Figure 4). In contrast, compounds **13**, **15**, and **17** favor the allosteric Site 2 (Figures 3C, 3D), partially overlapping with the binding sites of known TLR-7 antagonists MHV370 and E6732.[46,47] Thus, it was hypothesized that compounds **12**, **14**, **16**, **18 - 21** might act as agonists, binding similarly to either the TLR-7/8 agonist R848 or TLR-7 specific agonist CPG-52852 in Site 1. In contrast, compounds **13**, **15**, and **17** could be antagonists or allosteric modulators, binding Site 2 and overlapping with the TLR-7 antagonists MHV730 and E6742 (Figure 4B).

Interestingly, while known agonists R848 (**2**) and CPG-52852 both target site 1, they occupy different subregions, thus forming interactions with different sets of amino acid residues (Figures 3D, 4A, and 4C). This observation was mirrored by the docking results for the studied metabolites, which also bound in a similar fashion to each of the agonist within Site 1. While some derivatives closely mimic the interactions of R848 (**16**, **18 - 21**), the other (**14**) align with CPG-52852 (Figures 3C, 3D, 4A, and 4C). This suggests that these metabolites may exert their effects by engaging specific, distinct interaction networks within the same overall active site, potentially leading to subtly different functional outcome.

The distinct binding modes observed for R848 and CPG-52852 within the TLR8 orthosteric site (Site 1) may explain their different profiles. While both ligands occupy the same active site cavity due to the homology between TLR7 and TLR8, they engage in specific subregions and interact with different key amino acid (Figures 4A and 4C). As a dual TLR7/8 agonist, R848 presumably adopts a conformation within the TLR8 site that effectively induces the conformational changes required for receptor activation.[48] Conversely, being a specific TLR7 agonist, CPG-52852 binds to a distinct subregion within the TLR8 active site. Thus, the differences may correlate with the selectivity of these two agonists towards TLR7/8.

Importantly, compounds **13**, **15**, and **17** bind at sites 2 of the TLR-8 receptor, implying a mechanism of action different from orthosteric agonism, possibly involving antagonistic or allosteric modulation and warranting further study. Understanding this mechanism benefits targeted rational designs of TLR7/8 modulators with potentially distinct and more desirable profiles (e.g., antagonism or biased signaling) for immune-mediated conditions like EED-associated stunting.[17]

ISSN 2616-0684 (Print)
ISSN 2616-0692 (Electronic)

Table 8: The ADMET analysis for R848 (**2**) and its derivatives (**12-21**)

Ligands	Ames toxicity	herG I Inhibitor	herG II Inhibitor	Carcino genicity	Oral Rat Acute Toxicity (LD50)	Organic Cation Trans-porter	GI Absorp-tion	CYP inhibitory promiscuity	Cac0-2 Permeability	P-Glyco-protein Substrate	P-Glyco-protein Inhibitor	CYP 1A2 Inhibitor	CYP 2C19 Inhibitor	CYP 2C9 Inhibitor	CYP 3A4 Inhibitor	CYP 2D6 Inhibitor	CYP 2D6 Substrate	CYP 2C9 Substrate	CYP 3A4 Substrate
R848, (**2**)	Yes	No	Yes	No	2.413	No	94.304	0.5925	1.375	Yes	No	Yes	No	No	No	No	No	No	No
R848-El (**12**)	Yes	No	No	No	2.467	No	92.58	0.561	1.054	Yes	No	Yes	No	No	No	No	Yes	No	No
R848-Nox (**13**)	Yes	No	Yes	No	2.719	No	87.123	0.7537	-0.108	Yes	No	Yes	No	No	No	No	Yes	No	Yes
R848-Mod (**14**)	Yes	No	Yes	No	2.544	No	92.263	0.925	1.475	Yes	No	Yes	Yes	No	No	No	No	No	No
R848-ODet, (**15**)	Yes	No	Yes	No	2.65	No	80.359	0.606	-0.179	Yes	No	Yes	No	No	No	No	No	No	No
R848-ODetHyd, (**16**)	Yes	No	No	No	2.626	No	69.868	0.6561	-0.25	Yes	No	No	No	No	No	No	No	No	No
R848-Gluc, (**17**)	No	No	No	No	2.482	No	31.995	0.746	-0.652	Yes	No	No	No	No	No	No	No	No	No
R848-HydOx, (**18**)	No	No	No	No	2.47	No	55.977	0.628	-0.179	Yes	No	No	No	No	No	No	No	No	No
R848-ArHyd, (**19**)	Yes	No	No	No	2.446	No	80.183	0.5804	0.73	Yes	No	Yes	No	No	No	No	No	No	No
R848-Sulf, (**20**)	No	No	No	No	2.473	No	44.156	0.605	-0.634	Yes	No	No	No	No	No	No	No	No	No
R848-NOx, (**21**)	Yes	No	Yes	No	2.348	No	93.969	0.5336	0.937	Yes	No	Yes	No	No	No	No	No	No	No

ISSN 2616-0684 (Print)
ISSN 2616-0692 (Electronic)

Table 9: Binary system analysis for R848 (2) and its derivatives (**12-21**)

Ligands	**Ames toxicity**	**herG I Inhibitor**	**herG II Inhibitor**	**Carcinogenicity**	**Oral Rat Acute Toxicity (LD50)**	**Organic Cation Transporter**	**GI Absorption**	**CYP inhibitory promiscuity**	**Cac0-2 Permeability**	**P-Glycoprotein Substrate**	**P-Glycoprotein Inhibitor**	**CYP1A2 Inhibitor**	**CYP 2C19 Inhibitor**	**CYP 2C9 Inhibitor**	**CYP 3A4 Inhibitor**	**CYP 2D6 Inhibitor**	**CYP 2D6 Substrate**	**CYP 2C9 Substrate**	**CYP3A4 Substrate**
R848, (**2**)	0	1	0	1	1	1	1	0	1	0	1	0	1	1	1	1	1	1	1
R848-El (**12**)	0	1	1	1	1	1	1	0	1	0	1	0	1	1	1	1	0	1	1
R848-Nox (**13**)	0	1	0	1	1	1	1	0	0	0	1	0	1	1	1	1	0	1	0
R848-Mod (**14**)	0	1	0	1	1	1	1	0	1	0	1	0	0	1	1	1	1	1	1
R848-ODet, (**15**)	0	1	0	1	1	1	1	0	0	0	1	0	1	1	1	1	1	1	1
R848-ODetHyd, (**16**)	0	1	1	1	1	1	0	0	0	0	1	1	1	1	1	1	1	1	1
R848-Gluc, (**17**)	1	1	1	1	1	1	0	0	1	0	1	1	1	1	1	1	1	1	1
R848-HydOx, (**18**)	1	1	1	1	1	1	0	0	0	0	1	1	1	1	1	1	1	1	1
R848-ArHyd, (**19**)	0	1	1	1	1	1	1	0	1	0	1	0	1	1	1	1	1	1	1
R848-Sulf, (**20**)	1	1	1	1	1	1	0	0	1	0	1	1	1	1	1	1	1	1	1
R848-NOx, (**21**)	0	1	0	1	1	1	1	0	1	0	1	0	1	1	1	1	1	1	1
	N0 = 1 Yes = 0	No = 1 Yes = 0	No = 1 Yes = 0	No = 1 Yes = 0	>1 = 1 <1 = 0	No= 1 Yes=0	> 70 = 1 < 70 = 0	> 1 = 1 < 1 = 0	> 0.5 = 1 < 0.5 = 0	No = 1 Yes = 0	No = 1 Yes = 0	No = 1 Yes = 0	No = 1 Yes = 0	No = 1 Yes = 0	No = 1 Yes = 0	No = 1 Yes = 0	No = 1 Yes = 0	No = 1 Yes = 0	No = 1 Yes = 0

ISSN 2616-0684 (Print)
ISSN 2616-0692 (Electronic)

Table 10: ADMET score of 18 endpoints analysis of R848 (**2**) and its derivatives (**12-21**)

Ligands	Ames toxicity	herG I Inhibitor	herG II Inhibitor	Carcinogenicity	Oral Rat Acute Toxicity (LD50)	Organic Cation Trans-porter	GI Absorption	CYP inhibitory promiscuity	Cac0-2 Permeability	P-Glyco-protein Substrate	P-Glyco-protein Inhibitor	CYP1A2 Inhibitor	CYP 2C19 Inhibitor	CYP 2C9 Inhibitor	CYP 3A4 Inhibitor	CYP 2D6 Inhibitor	CYP 2D6 Substrate	CYP 2C9 Substrate	CYP 3A4 Substrate	ADMET SCORE
R848, (**2**)	0	0.4059	0	1	0.5867	0.2564	0.7548	0	0.3074	0	0.3735	0	0.2685	0.2633	0.2691	0.2829	0.2829	0.2633	0.2691	0.29
R848-El (**12**)	0	0.4059	0.4059	1	0.5867	0.2564	0.7548	0	0.3074	0	0.3735	0	0.2685	0.2633	0.2691	0.2829	0	0.2633	0.2691	0.30
R848-Nox (**13**)	0	0.4059	0	1	0.5867	0.2564	0.7548	0	0	0	0.3735	0	0.2685	0.2633	0.2691	0.2829	0	0.2633	0	0.25
R848-Mod (**14**)	0	0.4059	0	1	0.5867	0.2564	0.7548	0	0.3074	0	0.3735	0	0	0.2633	0.2691	0.2829	0.2829	0.2633	0.2691	0.28
R848-ODet, (**15**)	0	0.4059	0	1	0.5867	0.2564	0.7548	0	0	0	0.3735	0	0.2685	0.2633	0.2691	0.2829	0.2829	0.2633	0.2691	0.28
R848-ODetHyd, (**16**)	0	0.4059	0.4059	1	0.5867	0.2564	0	0	0	0	0.3735	0.2379	0.2685	0.2633	0.2691	0.2829	0.2829	0.2633	0.2691	0.27
R848-Gluc, (**17**)	0.6021	0.4059	0.4059	1	0.5867	0.2564	0	0	0.3074	0	0.3735	0.2379	0.2685	0.2633	0.2691	0.2829	0.2829	0.2633	0.2691	0.32
R848-HydOx, (**18**)	0.6021	0.4059	0.4059	1	0.5867	0.2564	0	0	0	0	0.3735	0.2379	0.2685	0.2633	0.2691	0.2829	0.2829	0.2633	0.2691	0.30
R848-ArHyd, (**19**)	0	0.4059	0.4059	1	0.5867	0.2564	0.7548	0	0.3074	0	0.3735	0	0.2685	0.2633	0.2691	0,282	0.2829	0.2633	0.2691	0.32
R848-Sulf, (**20**)	0.6021	0.4059	0.4059	1	0.5867	0.2564	0	0	0.3074	0	0.3735	0.2379	0.2685	0.2633	0.2691	0.2829	0.2829	0.2633	0.2691	0.32
R848-NOx, (**21**)	0	0.4059	0	1	0.5867	0.2564	0.7548	0	0.3074	0	0.3735	0	0.2685	0.2633	0.2691	0.2829	0.2829	0.2633	0.2691	0.29

Key findings and implications

Often linked to environmental enteric dysfunction (EED), childhood stunting represents a significant global health challenge characterized by chronic gut inflammation and immune dysregulation.[18] Toll-like receptors 7 and 8 (TLR7/8) regulate innate immunity and have emerged as relevant immunomodulatory targets. However, modulation of TLR7/8 poses a complex challenge with broad agonism having yielded detrimental immunological responses.[49] A good example is the complex immunological outcomes that resulted from the *ex vivo* use of TLR7/8 agonists in critically ill and undernourished children.[17] Collectively, they underscore the critical need for developing precisely tuned ligands capable of eliciting specific, beneficial immune effects without exacerbating inflammation or disrupting immune homeostasis particularly in vulnerable populations.

The challenge to find specific TLR7/8 modulators lies in the exploration of alternative modulation strategies, particularly selective antagonists or allosteric modulators. This approach aligns with successful drug development trends in other immune-mediated diseases. For instance, specific TLR7/8 antagonists (e.g., MHV370, E6732, afimetoran) are progressing through clinical trials for autoimmune conditions like lupus,[46,47] demonstrating the feasibility of targeted TLR7/8 inhibition. Furthermore, allosteric modulators, which bind to sites distinct from the orthosteric active site, theoretically offer greater potential for receptor subtype selectivity and fine-tuned signaling outcomes, potentially leading to improved safety profiles compared to orthosteric ligands.[50] Thus, identifying TLR7/8 antagonists or allosteric modulators represents a promising therapeutic strategy for conditions like EED-associated stunting.

Thus, the present study employed a structure-based *in silico* approach to investigate potential TLR7/8 modulators derived from the imidazoquinolinone scaffold of the known agonist R848. Molecular docking simulations assessed the binding interactions of various derivatives (compounds **12 - 21**) with TLR7/8 receptor. While most derivatives (compounds **12**, **14**, **16**, **18 - 21**) docked preferentially at the canonical orthosteric agonist binding site, three compounds (**13**, **15**, and **17**) exhibited a distinct preference for binding at a known allosteric site (Site 2). Notably, this allosteric site is also recognized as the binding location for established TLR7/8 antagonists such as MHV370 and E6732.[31]

The predicted allosteric binding of compounds **13**, **15**, and **17** to TLR-7/8 suggests that they may function differently from R848 and its orthosteric derivatives (compounds **16**, **18 - 21**). It is known that allosteric modulation can alter receptor conformation and signaling indirectly, potentially leading to antagonism or biased signaling pathways distinct from full agonism. This finding is particularly relevant given the complex responses observed with TLR7/8 agonists in undernourished children.[17] We hypothesized that compounds interacting with the allosteric site, like **13**, **14**, **15**, and **17**, might offer a solution to discover TLR-7/8 modulators with safer immunological profiles for treating stunting or other immune dysfunction.

While the present results are encouraging, significant future work is required. It is crucial to elucidate the precise downstream effects of modulating TLR7/8 (via antagonism or allosteric mechanisms) within the specific immunological context of stunting and EED. This approach necessitates investigating impacts on specific immune cell populations, cytokine profiles (e.g., NF-κB, IRF, Type I IFN pathways), and potential biomarkers of response in relevant *in vitro* and *ex vivo* systems using cells from target populations. Subsequently, *in vivo* studies in appropriate animal models are essential to evaluate efficacy (e.g., impact on growth, gut inflammation) and safety, carefully considering potential species differences in TLR7/8 responses. Exploring combinations with nutritional interventions may also yield synergistic benefits.

It is also imperative to acknowledge the limitations of this computational study. While providing valuable scientific data, *in silico* predictions (e.g., via ADMET Score, Drug Likeness, MetaTox) do not guarantee *in vivo* activity or safety profiles. These findings require rigorous experimental validation through biochemical assays, cell-based studies, and eventually animal models. The translation of these findings to clinical application requires overcoming these hurdles and directly assessing efficacy and safety in human populations affected by stunting.

To this end, this study identified novel imidazoquinolinone derivatives (e.g., **13**, **15**, and **17**), predicted to bind preferentially to an allosteric site on TLR7/8. Increasing evidence and this finding suggest that targeted allosteric modulation of TLR7/8 may represent a viable strategy to overcome the challenges associated with broad agonism, offering a potentially safer and more specific approach to addressing the immune dysfunction underlying EED and stunting. Although, validation remains essential, compounds **13**, **14**, **15**, and **17** show promise as immunomodulatory candidates, warranting further *in vitro* and *in vivo* investigations to potentially tackle the unmet medical issue of stunting.

Conclusion

The findings from the present study suggest that caulerpin inspired compounds offer a promising avenue for developing novel immunomodulators targeting TLR-7/8 to address immune dysfunction associated with stunting. Molecular docking studies revealed that caulerpin binds TLR-7/8 with high affinity. However, while initial drug-likeness assessment indicated suboptimal pharmacological properties, subsequent *in silico* screening and modification led to the identification of novel imidazoquinolinone derivatives with enhanced drug-like characteristics and predicted immunomodulatory activity particularly for compounds **13**, **15**, and **17** which bind to allosteric site and potentially exert different pharmacological outcome compared to their parent molecules. Nevertheless, the computational nature of this study necessitates careful consideration of potential off-target effects and calls for further investigation through *in vitro* and *in vivo* studies to validate these findings and fully elucidate the long-term safety and efficacy of these compounds. By developing therapeutic strategies tailored to these populations, particularly compounds **13**, **14**, **15**, and **17**, TLR-7/8 modulators can contribute to tackle the unmet global health challenge.

Conflict of Interest

The author`s declare no conflict of interest.

Author's Declaration

The authors hereby declare that the work presented in this article is original and that any liability for claims relating to the content of this article will be borne by them.

Acknowledgments

The authors are grateful to the Center for Research and Community Service of Politeknik Negeri Nusa Utara for providing administrative support throughout this project.

References

1. Khani Jeihooni A, Mohammadkhah F, Razmjouie F, Harsini PA, Sedghi Jahromi F. Effect of Educational Intervention Based on Health Belief Model on Mothers Monitoring Growth of 6–12 Months Child with Growth Disorders. BMC Pediatr. 2022; 22(1):1–11.
2. Tzioumis E, Kay MC, Bentley ME, Adair LS. Prevalence and Trends in the Childhood Dual Burden of Malnutrition in Low- and Middle-Income Countries, 1990-2012. Public Health Nutr. 2016; 19(8):1375–1388.
3. Surono IS, Jalal F, Bahri S, Romulo A, Kusumo PD, Manalu E, Yusnita, Venema K. Differences in Immune Status and Fecal SCFA Between Indonesian Stunted Children and Children with Normal Nutritional Status. PLoS One. 2021; 16(7):1–14.
4. Quamme SH and Iversen PO. Prevalence of Child Stunting in Sub-Saharan Africa and Its Risk Factors. Clin Nutr Open Sci. 2022; 42:49–61.

5. World Health Organization. WHO. Global Nutrition Targets 2025: Stunting Policy Brief. 2014. Available from: https://www.who.int/publications/i/item/WHO-NMH-NHD-14.3
6. UNICEF, WHO, World Bank Group. Levels and Trends in Child Malnutrition: UNICEF/WHO/The World Bank Group Joint Child Malnutrition Estimates: Key Findings of the 2021 Edition. 2021. Available from: https://www.who.int/publications/i/item/9789240025257
7. de Onis M and Branca F. Childhood Stunting: A Global Perspective. Matern Child Nutr. 2016; 12:12–26.
8. Bourke CD, Berkley JA, Prendergast AJ. Immune Dysfunction as a Cause and Consequence of Malnutrition. Trends Immunol. 2016; 37(6):386–398.
9. Gharpure R, Mor SM, Viney M, Hodobo T, Lello J, Siwila J, Dube K, Robertson R, Mutasa K, Berger C, Hirai M, Brown T, Ntozini R, Evans C, Hoto P, Smith L, Tavengwa N, Joyeux M, Humphrey J, Berendes D, Prendergast A. A One Health Approach to Child Stunting: Evidence and Research Agenda. Am J Trop Med Hyg. 2021; 104(5):1620–1624.
10. Firmansyah RRT, Murti B, Prasetya H. A Meta-Analysis of Correlation Between Diarrhea and Stunting in Children Under Five. J Epidemiol Public Health. 2023; 8(1):88–97.
11. Kraemer K. The Stunting Enigma. Sight Life. 2013; 27(2):12–16.
12. Smith LE, Stoltzfus RJ, Prendergast A. Food Chain Mycotoxin Exposure, Gut Health, and Impaired Growth: A Conceptual Framework. Adv Nutr. 2012; 3(4):526–531.
13. Hossain M, Nahar B, Haque MA, Mondal D, Mahfuz M, Naila NN, Gazi M, Hasan M, Haque N, Haque R, Arndt M, Walson J, Ahmed T. Serum Adipokines, Growth Factors, and Cytokines Are Independently Associated with Stunting in Bangladeshi Children. Nutrients. 2019; 11(8):1753.
14. Xia X, Hao H, Zhang X, Wong IN, Chung SK, Chen Z, Xu B, Huang R. Immunomodulatory Sulfated Polysaccharides from *Caulerpa racemosa* var. *peltata* Induces Metabolic Shifts in NF-κB Signaling Pathway in RAW 264.7 Macrophages. Int J Biol Macromol. 2021; 182:321–332.
15. Lucena AMM, Souza CRM, Jales JT, Guedes PMM, De Miranda GEC, de Moura AMA, Araujo-Junior J, Nascimento G, Scortecci K, Santos B, Souto J. The Bisindole Alkaloid Caulerpin, From Seaweeds of the Genus *Caulerpa*, Attenuated Colon Damage in Murine Colitis Model. Mar Drugs. 2018; 16(9):319.
16. Nagappan T and Vairappan CS. Nutritional and Bioactive Properties of Three Edible Species of Green Algae, Genus *Caulerpa* (Caulerpaceae). J Appl Phycol. 2014; 26(2):1019–1027.
17. Uebelhoer LS, Gwela A, Thiel B, Nalukwago S, Mukisa J, Lwanga C, Getonto J, Nyatichi E, Dena G, Makazi A, Mwaringa S, Mupere E, Berkley J, Lancioni C. Toll-Like Receptor-Induced Immune Responses During Early Childhood and Their Associations with Clinical Outcomes Following Acute Illness Among Infants in Sub-Saharan Africa. Front Immunol. 2022; 12:805216.
18. Sturgeon JP, Njunge JM, Bourke CD, Gonzales GB, Robertson RC, Bwakura-Dangarembizi M, Berkley J, Kelly P, Prendergast A. Inflammation: The Driver of Poor Outcomes Among Children with Severe Acute Malnutrition? Nutr Rev. 2023; 81(12):1636–1652.
19. Dallakyan S and Olson AJ. Small-Molecule Library Screening by Docking with PyRx. In: Hempel JE, Williams CH, Hong CC, editors. Chemical Biology: Methods and Protocols. New York, NY: Springer New York; 2015:243–250.
20. Zheng J, Xiong H, Li Q, He L, Weng H, Ling W, Wang D. Protocatechuic Acid from Chicory Is Bioavailable and Undergoes Partial Glucuronidation and Sulfation in Healthy Humans. Food Sci Nutr. 2019; 7(9):3071–3080.
37. Liang SC, Xia YL, Hou J, Ge GB, Zhang JW, He YQ, Wang J, Qi X, Yang L. Methylation, Glucuronidation, and
21. Zoete V, Daina A, Bovigny C, Michielin O. SwissSimilarity: A Web Tool for Low to Ultra High Throughput Ligand-Based Virtual Screening. J Chem Inf Model. 2016; 56(8):1399–1404.
22. Yang M, Larson PG, Brown L, Schultz JR, Kucaba TA, Griffith TS, Ferguson D. Toll-Like Receptor 7 and 8 Imidazoquinoline-Based Agonist/Antagonist Pairs. Bioorg Med Chem Lett. 2022; 59:128548.
23. Keppler M, Straß S, Geiger S, Fischer T, Späth N, Weinstein T, Schwamborn A, Guezguez J, Guse J, Laufer S, Burnet M. Imidazoquinolines With Improved Pharmacokinetic Properties Induce a High IFNα to TNFα Ratio *In Vitro* and *In Vivo*. Front Immunol. 2023; 14:1143896.
24. Rudik A, Bezhentsev V, Dmitriev A, Lagunin A, Filimonov D, Poroikov V. Metatox - Web Application for Generation of Metabolic Pathways and Toxicity Estimation. J Bioinform Comput Biol. 2019; 17(1):1940003.
25. Guan L, Yang H, Cai Y, Sun L, Di P, Li W, Liu G, Tang Y. ADMET-Score - A Comprehensive Scoring Function for Evaluation of Chemical Drug-Likeness. Medchemcomm. 2019 Jan; 10(1):148–157.
26. Discovery Studio 3.5. San Diego: Accelrys; 2017.
27. Lagunin A, Stepanchikova A, Filimonov D, Poroikov V. PASS: Prediction of Activity Spectra for Biologically Active Substances. Bioinformatics. 2000; 16(8):747–748.
28. Brown GJ, Cañete PF, Wang H, Medhavy A, Bones J, Roco JA, He Y, Qin Y, Cappelo J, Ellyard J, Bassett K, Shen Q, Burgio G, Zhang Y, Turnbull C, Meng X, Wu P, Cho E, Miosge L, Andrews T, Field M, Tvorogov D, Lopez A, Babon J, Lopez C, Gonzalez-Murillo A, Garulo D, Pascual V, Levy T, Mallack E, Calame D, Lotze T, Lupski J, Ding H, Ullah T, Walters G, Koina K, Cook M, Shen N, de Lucas Collantes C, Corry B, Gantier M, Athanasopoulos V, Vinuesa C. TLR7 Gain-of-Function Genetic Variation Causes Human Lupus. Nature. 2022; 605(7909):349–356.
29. Zheng H, Wu P, Bonnet PA. Recent Advances on Small-Molecule Antagonists Targeting TLR7. Molecules. 2023; 28(2):494.
30. Patinote C, Karroum NB, Moarbess G, Cirnat N, Kassab I, Bonnet PA, Deleuze-Masquefa C. Agonist and Antagonist Ligands of Toll-Like Receptors 7 and 8: Ingenious Tools for Therapeutic Purposes. Eur J Med Chem. 2020; 193:112238.
31. Zhang Z, Ohto U, Shibata T, Taoka M, Yamauchi Y, Sato R, Shukla N, David S, Isobe T, Miyake K, Shimizu T. Structural Analyses of Toll-Like Receptor 7 Reveal Detailed RNA Sequence Specificity and Recognition Mechanism of Agonistic Ligands. Cell Rep. 2018; 25(12):3371–3381.e5.
32. National Center for Biotechnology Information. PubChem Compound Summary for CID 10309114, Cpg-52852. National Center for Biotechnology Information. 2025. Available from: https://pubchem.ncbi.nlm.nih.gov/compound/Cpg-52852
33. Engel AL, Holt GE, Lu H. The Pharmacokinetics of Toll-Like Receptor Agonists and the Impact on the Immune System. Expert Rev Clin Pharmacol. 2011; 4(2):275–289.
34. Järvinen E, Deng F, Kiander W, Sinokki A, Kidron H, Sjöstedt N. The Role of Uptake and Efflux Transporters in the Disposition of Glucuronide and Sulfate Conjugates. Front Pharmacol. 2022; 12:822452.
35. Docampo-Palacios ML, Alvarez-Hernández A, Adiji O, Gamiotea-Turro D, Valerino-Diaz AB, Viegas LP, Ndukwe I, De Fatima A, Heiss C, Azadi P, Pasinetti G, Dixon R. Glucuronidation of Methylated Quercetin Derivatives: Chemical and Biochemical Approaches. J Agric Food Chem. 2020; 68(50):14790–14807.
36. Vitku J, Hill M, Kolatorova L, Kubala Havrdova E, Kancheva R. Steroid Sulfation in Neurodegenerative Diseases. Front Mol Biosci. 2022; 9:827018.

Sulfonation of Daphnetin in Human Hepatic Preparations *In Vitro*: Metabolic Profiling, Pathway Comparison, and Bioactivity Analysis. J Pharm Sci. 2016; 105(2):808–816.
38. Teles YCF and De Souza MSFV. Sulphated Flavonoids: Biosynthesis, Structures, and Biological Activities. Molecules. 2018; 23(2):475.
39. Williamson G, Kay CD, Crozier A. The Bioavailability, Transport, and Bioactivity of Dietary Flavonoids: A Review from a Historical Perspective. Compr Rev Food Sci Food Saf. 2018; 17(15):1054–1112.
40. Balansa W, Riyanti, Balansa KH, Hanif N. Harnessing the Ecofriendly Antifouling Potential of Agelasine Alkaloids Through MetaTox Analysis and Computational Studies. Trop J Nat Prod Res. 2025; 9(1):329–340.
41. Balansa W, Rieuwpassa FJ, Hanif N. Harnessing Ecofriendly Antifouling of Agelasine Alkaloids. Kamiya Jaya Aquatic; 2025.
42. Wang KP, Neumann C, Epp A, Zeng W, Griffith T, Ferguson D, Gardai S, Smith A. Generation of an Antibody-Drug Conjugate-Optimized TLR 7/8 Agonist Payload. Cancer Res. 2023; 83(7 Suppl):1542–1542.
43. Tojo S, Zhang Z, Matsui H, Tahara M, Ikeguchi M, Kochi M, Kamada M, Shigematsu H, Tsutsumi A, Adachi N, Shibata T, Yamamoto M, Kikkawa M, Senda T, Isobe Y, Ohto U, Shimizu T. Structural Analysis Reveals TLR7 Dynamics Underlying Antagonism. Nat Commun. 2020; 11(1):5015.
44. Ohto U, Tanji H, Shimizu T. Structure and Function of Toll-Like Receptor 8. Microbes Infect. 2014; 16(4):273–282.
45. Gies JP and Landry Y. 4 - Drug Targets: Molecular Mechanisms of Drug Action. In: Wermuth CG, editor. The Practice of Medicinal Chemistry (Second Edition). London: Academic Press; 2003:51–65.
46. Ishizaka ST, Hawkins L, Chen Q, Tago F, Yagi T, Sakaniwa K, Zhang Z, Shimizu T, Shirato M. A Novel Toll-Like Receptor 7/8–Specific Antagonist E6742 Ameliorates Clinically Relevant Disease Parameters in Murine Models of Lupus. Eur J Pharmacol. 2023; 957:175962.
47. Chiney M, Girgis I, Harrison M, Zhang X, Shen Y, Dawes M, Dong L, Shevell D, Aras U, Murthy B. BMS-986256, an Oral Novel Toll-Like Receptor 7 and 8 (TLR7/8) Inhibitor, Does Not Affect the Pharmacokinetics of Mycophenolate Mofetil in Healthy Subjects. Arthritis Rheumatol. 2021; 73(9):3686–3688.
48. Weeratna RD, Makinen SR, McCluskie MJ, Davis HL. TLR Agonists as Vaccine Adjuvants: Comparison of CpG ODN and Resiquimod (R-848). Vaccine. 2005; 23(45):5263–5270.
49. Hu A, Sun L, Lin H, Liao Y, Yang H, Mao Y. Harnessing Innate Immune Pathways for Therapeutic Advancement in Cancer. Signal Transduct Target Ther. 2024; 9(1):68.
50. Chen CJ, Jiang C, Yuan J, Chen M, Cuyler J, Xie XQ, Feng Z. How Do Modulators Affect the Orthosteric and Allosteric Binding Pockets? ACS Chem Neurosci. 2022; 13(7):959–977.
51. Tanji H, Ohto U, Shibata T, Miyake K, Shimizu T. Structural Reorganization of the Toll-Like Receptor 8 Dimer Induced by Agonistic Ligands. Science (1979). 2013; 339(6126):1426–1429.
52. Patra MC, Achek A, Kim GY, Panneerselvam S, Shin HJ, Baek WY, Lee W, Sung J, Jeong U, Cho E, Kim W, Kim E, Suh C, Choi S. A Novel Small-Molecule Inhibitor of Endosomal TLRs Reduces Inflammation and Alleviates Autoimmune Disease Symptoms in Murine Models. Cells. 2020; 9(7):1676.